RESEARCH LETTER

Regulation and structure of YahD, a copper-inducible α/β serine hydrolase of *Lactococcus lactis* IL1403

Jacobo Martinez[1], Stefano Mancini[2], Eva Tauberger[1], Christoph Weise[1], Wolfram Saenger[1] & Marc Solioz[2]

[1]Department of Biology, Chemistry and Pharmacy, Free University of Berlin, Berlin, Germany; and [2]Department of Clinical Pharmacology, University of Berne, Berne, Switzerland

Correspondence: Marc Solioz, Department of Clinical Pharmacology, University of Berne, Murtenstrasse 35, 3010 Berne, Switzerland. Tel.: +41 31 632 3268; fax: +41 31 632 4997; e-mail: marc.solioz@ikp.unibe.ch

Received 23 August 2010; revised 8 October 2010; accepted 11 October 2010.
Final version published online 9 November 2010.

DOI:10.1111/j.1574-6968.2010.02144.x

Editor: Dieter Jahn

Keywords
copper homeostasis; α/β serine hydrolase; CopR regulon; crystal structure.

Abstract

Lactococcus lactis IL1403 is a lactic acid bacterium that is used widely for food fermentation. Copper homeostasis in this organism chiefly involves copper secretion by the CopA copper ATPase. This enzyme is under the control of the CopR transcriptional regulator. CopR not only controls its own expression and that of CopA, but also that of an additional three operons and two monocistronic genes. One of the genes under the control of CopR, *yahD*, encodes an α/β-hydrolase. *YahD* expression was induced by copper and cadmium, but not by other metals or oxidative or nitrosative stress. The three-dimensional structure of YahD was determined by X-ray crystallography to a resolution of 1.88 Å. The protein was found to adopt an α/β-hydrolase fold with the characteristic Ser-His-Asp catalytic triad. Functional testing of YahD for a wide range of substrates for esterases, lipases, epoxide hydrolases, phospholipases, amidases and proteases was, however, unsuccessful. A copper-inducible serine hydrolase has not been described previously and YahD appears to be a new functional member of this enzyme family.

Introduction

Lactococcus lactis IL1403 is a Gram-positive lactic acid bacterium used extensively in the manufacture of food, in the dairy industry and for an increasing number of biotechnological applications. Its genome has been sequenced (Bolotin *et al.*, 2001) and its proteome has been characterized (Guillot *et al.*, 2003). For these reasons, it represents a good model organism for molecular studies. In industrial processes, bacteria are often exposed to a variety of stress conditions, including extreme pH and temperature, osmotic shock and metal stress (van de Guchte *et al.*, 2002). For example, in the traditional production of Swiss cheese in copper vats, *L. lactis* is exposed to copper leaching from the vats.

Copper is an essential biological element for many organisms, but at elevated concentrations, it becomes toxic to cells. Because of its ability to cycle between Cu^{2+} and Cu^{+} at relevant biological redox potentials, copper has been adopted as a cofactor by >30 known enzymes (Karlin, 1993), such as lysyl oxidase, superoxide dismutase and cytochrome *c* oxidase (Linder & Hazegh Azam, 1996). On the other hand, the redox properties of copper can lead to the formation of toxic reactive oxygen species via a Fenton-type reaction, which may result in cellular damage (Magnani & Solioz, 2007). Recent findings suggest that an important *in vivo* toxicity mechanism of copper also consists of the displacement of iron from iron–sulfur clusters of proteins (Macomber & Imlay, 2009; Chillappagari *et al.*, 2010). Because of these potential toxic effects of copper, tight homeostatic control is pivotal for all organisms. Bacteria establish copper homeostasis chiefly by exporting excess copper and by sequestering cytoplasmic copper with copper chaperones for safe delivery to copper exporters and copper-requiring proteins (Solioz *et al.*, 2010). The genes involved in copper homeostasis are regulated by copper-responsive transcriptional regulators.

Lactococcus lactis has been used recently as a model organism for the study of bacterial copper homeostasis. It was found that a set of widely diverse genes are under the control of the CopR copper-responsive repressor (Magnani *et al.*, 2008). This so-called CopR regulon encompasses 14 genes: two monocistronic genes (*lctO*, *copB*) and four operons (*ydiDE*, *yahCD-yaiAB*, *ytjDBA* and *copRZA*). Some

FEMS MICROBIOLOGY LETTERS

of the proteins encoded by these genes, such as the CopR repressor, the CopZ copper chaperone and the two copper ATPases, CopA and CopB, play an evident role in copper homeostasis by dealing directly with copper ions (Solioz & Vulpe, 1996; Solioz & Stoyanov, 2003; Solioz *et al.*, 2011). Two more proteins of the CopR regulon have been studied in detail: LctO is a lactate oxidase that converts lactate to pyruvate under the use of molecular oxygen, presumably to reduce oxygen tension and thus oxygen-associated stress (Barré *et al.*, 2007). CinD, on the other hand, is a nitroreductase (encoded by *ytjD*) that can detoxify nitro compounds that exacerbate copper stress (Mermod *et al.*, 2010).

In the present study, we investigated the function of another member gene of the CopR regulon, *yahD*. By sequence comparison, this gene is predicted to encode an α/β serine hydrolase of 206 amino acids. The α/β-hydrolase fold is one of the most versatile and widespread folds known (Nardini & Dijkstra, 1999). Even though all the members of this superfamily have a similar fold and a conserved catalytic triad, they exhibit wide substrate specificity. Serine hydrolases use a nucleophilic serine to hydrolyze amidic, ester and thioester bonds in small molecules or proteins (Simon & Cravatt, 2010). YahD was found to be induced by copper, cadmium and silver, but not by other metals or by oxidative or nitrosative stress-inducing chemicals. The three-dimensional structure of YahD was resolved by X-ray crystallography to a resolution of 1.88 Å and was found to exhibit an α/β-hydrolase fold with the characteristic Ser-His-Asp catalytic triad. YahD did not catalyze any of the known α/β serine hydrolase reactions and appears to represent a novel subclass of serine hydrolases.

Materials and methods

Bacterial strains and culture conditions

Lactococcus lactis IL1403 was grown semi-anaerobically (air-saturated media in sealed bottles), in M17 media (Terzaghi & Sandine, 1975) at 30 °C or on plates containing M17 media with 1.5% agar (AppliChem, Darmstadt, Germany). *Escherichia coli* DH5α (Stratagene, La Jolla, CA) and ER2566 (Invitrogen life Technologies) cells used for cloning were transformed according to the manufacturer's instructions. *Escherichia coli* strains were cultivated aerobically at 37 °C in Luria–Bertani (LB) media (Sambrook *et al.*, 1989) with the appropriate antibiotics.

Construction of a YahD expression vector

All plasmids were purified from *E. coli* DH5α using the Large Scale Nucleobond® AX plasmid isolation kit (Macherey-Nagel, Oensingen, Switzerland). The *yahD* gene was PCR-amplified from genomic DNA of *L. lactis* IL1403, using the following primers: sm10 (5′-TGAATGGAGGAG GACATATGACAGATTATGTT; NdeI-site underlined) and sm11 (5′-TGCACTGAAACTTTTTCAATAC). The PCR product was inserted into the TOPO-TA cloning vector® (Invitrogen life Technologies), resulting in pTHB. The *yahD* gene was excised from pTHB with NdeI and NotI and ligated into the pTYB12 expression vector (IMPACT™-CN system, New England Biolabs), cut with the same enzymes, resulting in pSMI.

Purification of YahD

Escherichia coli Rosetta (Novagen, UK) transformed with pSMI was grown to the mid-log phase at 37 °C in LB broth containing 100 μg mL^{-1} ampicillin, cooled to 18 °C and induced with 1 mM isopropyl-β-D-thiogalactopyranoside. Following overnight growth, cells were harvested by centrifugation at 3000 ***g*** for 10 min at 4 °C. Cell pellets were resuspended in 10 mM Tris-Cl, 150 mM NaCl, 1 mM EDTA, pH 8.0, and frozen at − 20 °C. To the thawed cell suspension, a tablet of EDTA-free complete protease inhibitor cocktail (Roche, Switzerland) and 10 μg mL^{-1} of DNaseI (Roche) was added and cells were disrupted by three pressure cycles in an Emulsiflex C5 homogenizer (Avestin, Germany) at 1000–1500 bar at 4 °C. Debris was removed by centrifugation at 4 °C for 10 min at 3000 ***g***. The supernatant was centrifuged at 90 000 ***g*** for 30 min at 4 °C, filtered and YahD was absorbed to chitin beads (New England Biolabs) in the batch mode for 1 h at 4 °C. Intein cleavage was induced with 10 mM Tris-Cl, 150 mM NaCl, 1 mM EDTA and 50 mM dithiothreitol, pH 8.0, on a column. YahD-containing fractions eluted from the chitin column were concentrated on an Amicon-Ultra-10k centrifugal filter (Millipore) and further purified by size exclusion chromatography on a Superdex S-75 26/60 column (GE Healthcare, Germany) in 10 mM Tris-Cl, 150 mM NaCl and 1 mM EDTA, pH 8.0. Fractions were analyzed by electrophoresis on 12% sodium dodecylsulfate (SDS) polyacrylamide gels and stained with Coomassie blue as described (Laemmli & Favre, 1973). Fractions containing pure YahD were pooled and concentrated as before to 10 mg mL^{-1}. Protein concentrations were determined with the BioRad protein assay (BioRad, Richmond) using bovine serum albumin as a standard.

MS

The total masses of purified, native YahD as well as YahD incubated overnight with 0.1 mM phenylmethylsulfonylfluoride were analyzed by matrix-assisted laser desorption ionization-time of flight MS (MALDI-TOF-MS) using an Ultraflex-II TOF/TOF instrument (Bruker Daltonics, Bremen, Germany) equipped with a Smart beam™ laser. Sinapinic acid was used as a matrix.

Western blot analysis of YahD expression

Antibodies to YahD were raised by injecting rats with an initial subcutaneous injection of 100 μg of gel-purified, cleaved YahD, followed by six intravenous booster injections of 100 μg YahD each. Sera were coagulated overnight at 4 °C, and the clear supernatant was used for Western blotting. For this, cultures in 2 mL of M17 media were grown to an $OD_{546\,nm}$ of 0.6–0.8, followed by induction for 90 min with either 20 μM to 3 mM $CuSO_4$, 20 μM $AgNO_3$ or $CdSO_4$, 200 μM each of $ZnSO_4$, $FeSO_4$, $NiCl_2$, $CoCl_2$, nitrosoglutathione or H_2O_2, and 100 μM of 4-nitroquinoline-1-oxide. Cell lysates were prepared by centrifuging the cultures and treating the cell pellets with 50 μL of 10 mg mL^{-1} lysozyme, 1 mM EDTA and 10 mM Tris-Cl, pH 8, for 30 min at 37 °C. 10 μL of 1 mg mL^{-1} DNaseI in 100 mM $MgCl_2$ was added and incubation was continued for 10 min at 25 °C. Cell debris was removed by centrifugation for 5 min at 12 000 ***g***. Protein concentrations in the supernatants were determined using the BioRad protein assay and 50 μg of protein resolved by electrophoresis on 12% SDS polyacrylamide gels. Western blots were prepared as described previously (Towbin *et al.*, 1979), using a horseradish peroxidase-coupled goat anti-rat IgG secondary antibody (Santa Cruz). Bands were visualized by chemiluminescence using 100 mM Tris-Cl, pH 8.5, 1.25 mM 3-aminophtalhydrazide, 0.2 mM *p*-coumaric acid and 0.01% H_2O_2. Chemiluminescence signals were captured using a Fuji LAS-1000 imaging system (Fuji Photo Film, Tokyo, Japan).

Crystallization

The following commercial crystallization screens were used to look for initial crystallization conditions: Screen I and II (Hampton Research), JCSG (Jena Bioscience) and PACT (Qiagen GmbH, Hilden, Germany). Flat-bottomed multi-subwell plates (Greiner, Langenthal, Switzerland) were used to set up sitting drop vapor-diffusion experiments by mixing 1 μL of 10 mg mL^{-1} YahD solution with 1 μL of screening solution and incubating at 18 °C. Initial conditions that yielded crystals were optimized by hanging drop vapor diffusion crystallization. Needle-shaped crystals were grown by mixing 1.5 μL of protein solution with 1 μL of well solution containing 37.5% polyethylene glycol 3350 and 150 mM of Na-DL-malate, pH 7.0. Crystals grew to 50 μm in the longest direction within 3 weeks. For data collection, crystals were flash-frozen in liquid nitrogen without the addition of a cryoprotectant. The crystals belonged to the orthorhombic space group $P2_12_12_1$, with unit cell dimensions of $a = 40.67$ Å, $b = 79.07$ Å and $c = 130.03$ Å.

Structure determination and model quality analysis

X-ray diffraction data were collected from a single crystal at beam line BL 14.1 at BESSY, Berlin, at 100 K and 0.918 Å wavelength. The data were integrated, reduced and scaled using XDS (Kabsch, 1993), resulting in a final data set that was fully complete at 1.88 Å resolution. A search model was built using the CCP4 suite program CHAINSAW (Stein, 2008), using the atomic coordinates of one monomer of the structure of the *Bacillus cereus* carboxylesterase (PDB accession 2HLI), which shares 32% amino acid identity with YahD. The sequence alignment of YahD to the *B. cereus* carboxylesterase, combined with the atomic coordinates of the latter protein, produced a final search model that did not contain water molecules and had the side chains cut after the β atom. Initial phases for the YahD crystal data were obtained by molecular replacement using MOLREP of the CCP4 program suite (Collaborative Computational Project, Number 4, 1994; Vagin & Teplyakov, 2010). The model obtained was subjected to rigid-body refinement, followed by iterative cycles of restrained-maximum likelihood refinement, including isotropic temperature factor adjustment with REFMAC (Murshudov *et al.*, 1997) and by manual rebuilding using COOT (Emsley & Cowtan, 2004). During this process, 5% randomly selected reflections have been used to calculate R_{free} to monitor bias during model building and refinement. Water molecules were added using COOT, and the validation of the model was carried out using MOLPROBITY. The atomic coordinates and structure factors have been deposited in the Protein Data Bank under accession 3OG9.

Results and discussion

Operon-organization and sequence comparison of YahD

We previously identified *yahD* as a copper-induced gene of *L. lactis* IL1403 and, here, aimed to characterize the corresponding gene product. By visual inspection and bioinformatics analysis (Ermolaeva *et al.*, 2001), the gene encoding YahD is predicted to be part of an operon consisting of *yahC*, *yahD*, *yaiA* and *yaiB* (Fig. 1). The operon is preceded by a *cop* box of consensus TACANNTGTA, which has been shown previously to interact with the copper-responsive repressor, CopR, of *L. lactis*. The operon terminates in a hairpin loop (theoretical stability −16.8 kcal), which presumably acts as a ρ-independent transcriptional terminator. The presence of these transcriptional control elements, together with the dense spacing of the four genes, further supports the operon structure.

The first gene of the operon, *yahC*, encodes a hypothetical protein of 65 amino acids (accession NP_835288), followed by *yahD* (accession NP_266234), predicted to encode a serine hydrolase of 206 amino acids. The final two genes of the operon are *yaiA* (accession NP_266233), encoding a predicted protein of 389 amino acids with sequence

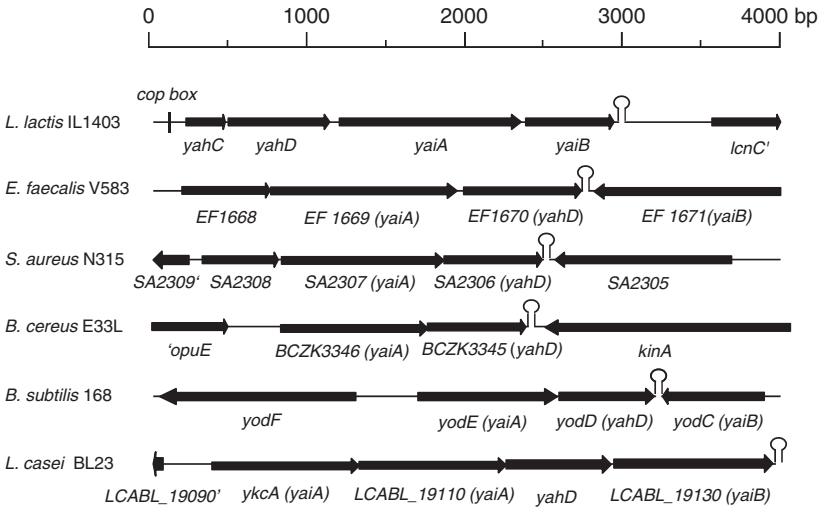

Fig. 1. Arrangement of operons containing *yahD*-like genes. The operons of *Lactococcus lactis* IL1403 (accession AE005176), *Enterococcus faecalis* V583 (accession AE016830), *Staphylococcus aureus* N315 (accession BA000018), *Bacillus cereus* E33L (accession CP000001), *Bacillus subtilis* 168 (accession AL009126) and *Lactobacilllus casei* BL23 (accession FM177140) are shown. The genes are drawn to scale and the position of the dyads is indicated by hairpin loops. The *cop* box is indicated by a vertical bar. The homology of genes to *L. lactis* genes is indicated in parentheses. *EF1668* and *SA2308* encode predicted regulatory proteins; other genes are described in the text.

similarity to glyoxylases I (lactoylglutathione lyases), and *yaiB* (accession NP_266234), encoding a hypothetical protein of 196 amino acids. All proteins of the operon have calculated pI values in the range of 4.5–5.

Because bacterial genes are usually grouped in operons based on metabolic relationships, we also studied the operon context of *yahD*-like genes in related organisms. The *L. lactis* operon and the operons of five other well-studied *Firmicutes*, namely *Enterococcus faecalis* V583, *Staphylococcus aureus* N315, *B. cereus* E33L, *Bacillus subtilis* 168 and *Lactobacillus casei* BL23, were compared (Fig. 1). All six operons feature the expected -10 and -35 sequence elements and are also terminated by stem–loop structures with stabilities of -10.9 to -27.7 kcal mol^{-1}. Interestingly, the *yahC* gene is unique to *L. lactis*, while the *yaiA* and *yahD* genes are conserved and are in the same operons in other analyzed organisms, most often forming a two-gene operon (*yaiA* is duplicated in *L. casei*). This suggests that *yahD* and *yaiA* encode proteins of the same or related biological pathways. In *E. faecalis* and *S. aureus*, these operons also encode a predicted regulator. The *yaiB* gene, on the other hand, is in the same operon only in *L. lactis* and *L. casei*, while it is present as an adjacent, divertantly transcribed gene in *E. faecalis* and *B. subtilis*. Based on sequence similarity, the *yaiA*-like genes shown in Fig. 1 have been annotated as putative glyoxylases. However, a direct demonstration of the function of any of these genes is not available.

YahD exhibits 31%, 32%, 34%, 32% and 42% sequence identity with the most homologous proteins aligned in Fig. 2. In all these proteins, there is a conserved catalytic triad typical of α/β serine hydrolases, characterized by Ser107, Asp157 and His188 of *L. lactis* YahD. The closest relative of this group of aligned proteins that has been characterized biochemically is EstB of *Pseudomonas fluorescence*. It shares 17% sequence identity with YahD of *L. lactis* and functions as a carboxylesterase with maximal hydrolytic activity towards (*p*-nitro)phenyl acetate (Hong *et al.*, 1991). Because α/β serine hydrolases are an extremely diverse family of enzymes, this does not imply a function for related enzymes.

Regulation of YahD expression by metal ions

To learn more about the function of YahD of *L. lactis* in copper homeostasis and stress response, we analyzed *in vivo* expression by Western blot analysis with an antibody against YahD. Expression was upregulated by copper, with maximal expression observed at 200 μM extracellular Cu^{2+} (Fig. 3). Among other metals tested, 20 μM Cd^{2+} induced YahD expression to even higher levels than copper, while Ag^{+} at the same concentration induced YahD only marginally. Zn^{2+}, Fe^{2+}, Ni^{2+} and Co^{2+} failed to stimulate YahD expression. Likewise, oxidative stress by 4-nitroquinoline-1-oxide or hydrogen peroxide and nitrosative stress by nitrosoglutathione failed to induce YahD. This induction specificity is typical for genes under the control of the CopR copper-inducible repressor and suggests that CopR is the sole regulator governing the expression of YahD. In line with this, Hg^{2+} and Pb^{2+} also failed to induce YahD (not shown).

Overexpression and purification or YahD

To functionally and structurally characterize YahD, the gene was cloned in an expression vector as a fusion protein with a chitin affinity tag, connected to the N-terminus of YahD via a self-cleaving intein. Self-cleavage of the intein with dithiothreitol resulted in YahD with Ala-Gly-His added to the N-terminal methionine. Preparations with $>$ 99% purity and of the expected apparent molecular weight of 23.6 kDa were routinely obtained with a yield of 2 mg L^{-1} of culture (Fig. 4). Purified YahD was highly soluble and stable when stored frozen at -80 °C.

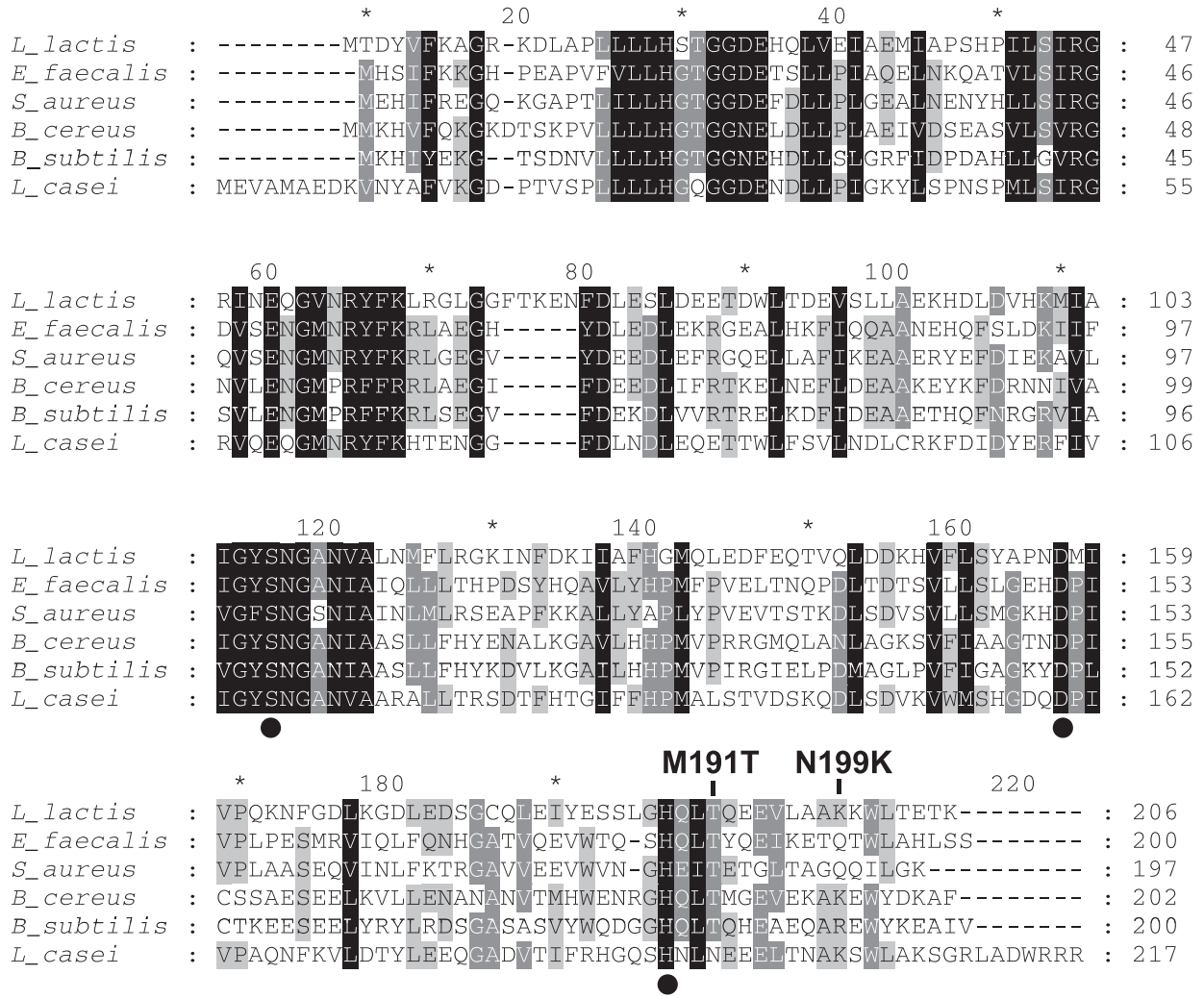

Fig. 2. Alignment of YahD of *Lactococcus lactis* with YahD-like sequences of other *Firmicutes*. The protein sequences were aligned with CLUSTALW and conserved amino acids are displayed in inverse type. *L_lactis*, YahD of *Lactococcus lactis* (this work); *E_faecalis*, predicted phospholipase/carboxylesterase of *Enterococcus faecalis* V583 (accession NP_815378); *S_aureus*, predicted phospholipase/carboxylesterase of *Staphylococcus aureus* N315 (accession NP_375630); *B_cereus*, predicted carboxylesterase of *Bacillus cereus* 14 579 (accession NP_833371.1); *B_subtilis*, predicted esterase of *Bacillus subtilis* 168 (accession NP_389837.1); *L_casei*, YahD of *Lactobacillus casei* BL23 (accession YP_001987849.1). Differences in the amino acid sequence of the gene isolated in this work compared with the annotated sequence NP_266232.1 are indicated above the *L. lactis* sequence. The large dots below the alignment indicate the three amino acids typical of α/β serine hydrolase catalytic sites.

Sequencing of the cloned *yahD* gene revealed two amino acid replacements, M191T and N199K, relative to the *L. lactis* genome sequence deposited in GenBank. The mass of purified YahD was measured by MALDI-TOF MS and found to be 23 578, which agrees, within experimental error, with the calculated mass of 23 575.3 for YahD with the extended N-terminus and the two amino acid replacements.

The two amino acid replacements in YahD were observed in two independently isolated clones from different PCR reactions and in different vectors. Moreover, the proteins most closely related to YahD of *L. lactis* contain T or N, but never M, at the position corresponding to T191 of *L. lactis* YahD. Likewise, the position corresponding to K199 of *L. lactis* YahD features K, Q or R, but not N, in the most closely related proteins (cf. Fig. 2). This suggests that the underlying cause of the two amino acid replacements in *L. lactis* YahD is not a cloning artifact, but sequence errors in the genome sequence of *L. lactis* deposited in GenBank under accession code NC_002662.

Determination of the YahD structure

The structure of YahD was determined by molecular replacement using *B. cereus* carboxylesterase atomic coordinates

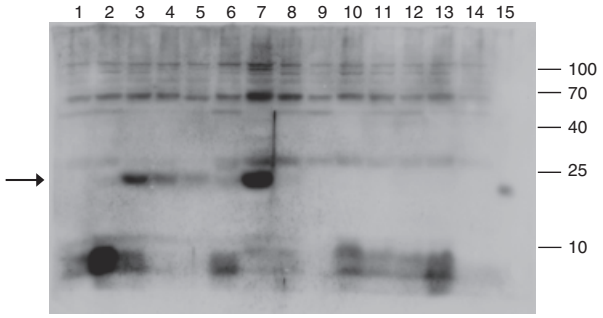

Fig. 3. *In vivo* expression of YahD in response to metal ions and stress conditions. Crude extracts of *Lactococcus lactis* IL1403 were separated by polyacrylamide gel electrophoresis, followed by Western blotting and development with a rat anti-YahD antibody. Lane 1, uninduced; lane 2, induced with 20 μM $CuSO_4$; lane 3, induced with 200 μM $CuSO_4$; lane 4, induced with 1 mM $CuSO_4$; lane 5, induced with 3 mM $CuSO_4$; lane 6, induced with 20 μM $AgNO_3$; lane 7, induced with 20 μM $CdSO_4$; lane 8, induced with 200 μM $ZnSO_4$; lane 9, induced with 200 μM $FeSO_4$; lane 10, induced with 200 μM $NiCl_2$; lane 11, induced with 200 μM $CoCl_2$; lane 12, induced with 100 μM 4-nitroquinoline-1-oxide; lane 13, induced with 200 μM nitrosoglutathione; lane 14, induced with 200 μM H_2O_2; lane 15, 5 ng of purified YahD. Molecular weights in kDa are indicated to the right of the gel and the arrow indicates the band corresponding to YahD.

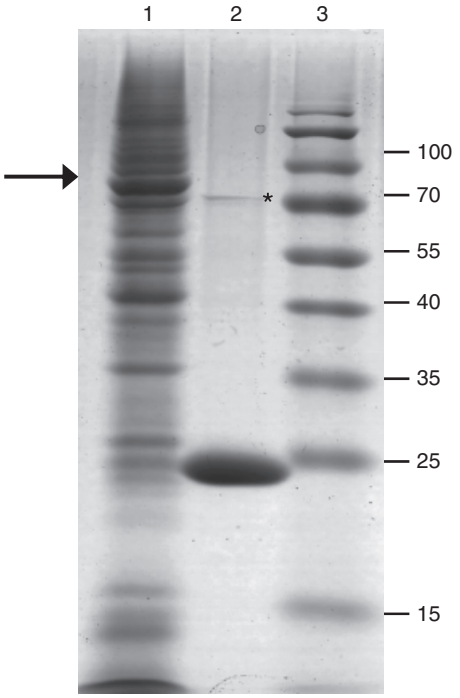

Fig. 4. Purification of YahD of *Lactococcus Lactis* IL1403. Proteins were resolved on a 12% SDS gel and stained with Coomassie blue. Lane 1, 50 μg of crude cytoplasmatic extract containing overexpressed YahD with the chitin-binding protein-intein tag (indicated by the arrow); lane 2, 5 μg of YahD, eluted with 50 mM dithiothreitol from the chitin column (some coeluting tag is indicated by an asteriks); lane 3, molecular weight markers, with the sizes in kDa indicated on the right.

as a search model as described in Materials and methods. The final refined model had a resolution of 1.88 Å and contained two monomers of YahD and 485 water molecules in the asymmetric unit. Each monomer contained all the 206 residues. A D-malic acid molecule from the crystallization buffer was located in the presumed active site. Because the electron density maps were of high quality, the two monomers of the asymmetric unit as well as the malic acid could be built reliably. The refinement statistics of the final model against all data in the resolution range of 40.00–1.88 are shown in Table 1. The absence of noncrystallographic symmetry and the examination of possible surface patches suitable for dimerization using PISA (Krissinel & Henrick, 2007) suggested that the wild-type enzyme exists as a monomer. This conclusion is in agreement with analytical gel filtration analysis (data not shown).

The average B factors for chain A (12.16 $Å^2$) and chain B (11.78 $Å^2$) show no significant difference. Similar values have been found for residues present in the presumed active site. In contrast, the mean temperature factor values for the bound malic acid molecules (21.0 $Å^2$ for chain A, 22.8 $Å^2$ for chain B) are nearly twice as large. This could be due to a lower occupancy of the ligand or to a higher agitation if it is considered that the mean B value for the solvent water molecules (23.64 $Å^2$) is higher than the B values for the malic acid ligand.

The superimposition of the two monomers present in the asymmetric unit shows that both chains have identical topographies and a root-mean-square deviation value of 0.43 Å. The torsion angles Ψ and φ of all the amino acids are

Table 1. Data collection and refinement statistics

Data set	Values
Space group	$P2_12_12_1$
Cell constants (Å)	$a = 40.67$, $b = 79.07$, $c = 130.03$
Resolution range (Å; last shell)	40–1.88 (1.93–1.88)*
Number of observations	307 703
Number of unique reflections	34 965
Completeness (%)	100 (100)*
I/sigma	15.91 (3.90)*
R merge (%)	13.9 (69.1)*
Refinement	
R_{work}	16.7 (20.3)*
R_{free}	22.68 (27.1)*
r.m.s. deviations (Å)	
Bond lengths	0.015
Bond angles	1.42
Average B factors ($Å^2$)	
Protein (Chain A/Chain B)	12.2/11.8
Ligand (Chain A/Chain B)	21.0/22.8
Waters	23.6

*Values in parentheses indicate values for the highest resolution shell
r.m.s. deviation, root-mean-square deviation.

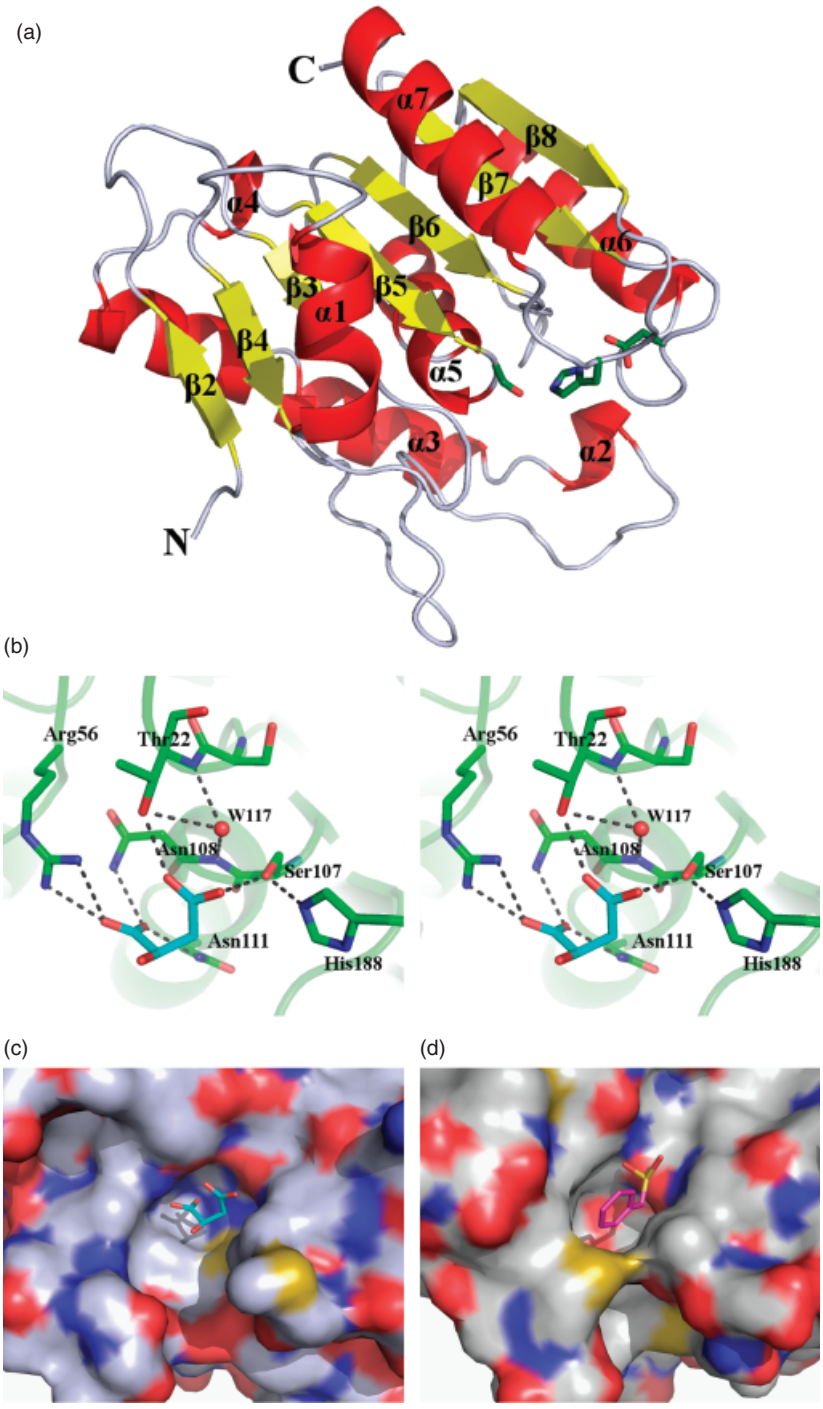

Fig. 5. (a) General view of YahD. Ribbon diagram of YahD showing the α/β hydrolase fold and the catalytic triad. The β-strands (yellow) and the α-helices (red) are numbered from β2 to β8 and from α1 to α7, respectively, to be consistent with the nomenclature from Ollis *et al*. (1992). The N- and C-termini are also indicated. The catalytic residues S107, H188 and D157 are shown as stick models. The YahD structure has been deposited in the Protein Data Base under accession 3OG9. (b) Stereo view of the active site of YahD. The D-malic acid molecule is shown in cyan and the surrounding residues are displayed as stick models. Hydrogen bonds between the ligand and the surrounding amino acids are shown as dashed lines. A water molecule (W117) occupying the position of the putative oxyanion hole and hydrogen bonded to the hydroxyl residue of Thr22 and the backbone nitrogens of Thr22and Asn108 is displayed as a red sphere. (c) Surface representation of the active site region of YahD with D-malic acid (cyan), and (d) of the carboxylesterase from *Pseudomonas fluorescens* with phenylmethylsulfonylfluoride (pink; PDB accession 1AUR). Surfaces of oxygen, nitrogen and sulfur atoms are displayed in red, blue and yellow, respectively.

located in the favorable regions of the Ramachandran plot. Only Ser39, Asn50, Thr67 and Ser107 are in the 'allowed' region. This is especially interesting for the catalytic site-residue Ser107 ($\Psi = -123.75$ $\varphi = 54.71$). A unique conformation of this active-site serine has been reported for other α/β serine hydrolases and has been termed the 'nucleophile elbow' (Ollis *et al*., 1992).

Overall structure of YahD

YahD is a monomeric globular protein, consisting of a central β-sheet composed of seven β-strands, surrounded by six α-helices (Fig. 5a). All strands of the central β-sheet are parallel, except for the first, N-terminal one. This fold can be classified as an α/β-hydrolase fold. The prototypic

α/β-hydrolase fold consists of an eight-stranded β-sheet in which all except the second β-stand are parallel. This central β-sheet exhibits a left-handed superhelical twist that positions the first and the last β-strand at an angle of approximately 90° to each other. YahD is lacking the first, N-terminal β-strand in comparison with the canonical α/β hydrolase fold. According to Ollis *et al.* (1992), this should not affect the catalytic activity because the first two β-strands of the prototypic α/β hydrolase fold are not directly involved in the formation of the active site. This notion is supported by the structures of the carboxylesterase of *Pseudomonas fluorescens* (Kim *et al.*, 1997) and the cutinase of *Aspergillus oryzae* (Liu *et al.*, 2009), which also lack the initial β-strand.

Catalytic triad, oxyanion hole and ligand binding

The α/β hydrolase fold-enzymes possess a catalytic triad consisting of a nucleophilic residue (serine, cysteine or aspartic acid), a histidine and an acidic residue. The crystal structure of YahD revealed that Ser107, His188 and Asp157 form this catalytic triad. Like most serine hydrolases, YahD possesses the conserved sequence motif Gly-X-Ser-X-Gly close to the active site serine (Brenner, 1988). This characteristic motif allows the reactive serine to adopt the characteristic nucleophile elbow. A well-defined patch of electron density close to Ser107 could unambiguously be attributed to a D-malic acid molecule; this molecule had been specifically acquired from the crystallization buffer, which contained a racemic DL–malic acid mixture. The nucleophilic Ser107 points to one oxygen atom of the carboxyl group of the D-malic acid (Fig. 5b). The bottom of the binding pocket is formed mainly by hydrophilic residues (Thr22, Arg56, Asn108, Asn111), which form hydrogen bonds with malic acid. This suggests that YahD will prefer a polar substrate molecule over a lipophilic one. The reaction mechanism of serine hydrolases involves a nucleophilic attack of a carboxylic carbon by the active-site serine, producing an acyl-intermediate with a negatively charged oxygen. To stabilize this charge, an oxyanion hole is present in the active site. The position of this hole is most likely delineated by the water molecule (W117), which was located close to Ser107 and in hydrogen bond-distance to the Thr22 and Asn108 backbone-nitrogen atoms. A surface representation of the active site shows that it is wide open and possibly accessible to large substrates (Fig. 5c). This contrasts with the less accessible active sites of some other serine hydrolases, such as the carboxylesterase from *P. fluorescens* (Fig. 5d).

YahD function

Phenylmethylsulfonylfluoride is a common inhibitor of serine hydrolases and binds covalently to the active serine. To verify the nucleophilic serine residue of YahD, it was incubated with phenylmethylsulfonylfluoride, followed by MALDI-TOF MS. A new peak with a mass gain of +161 (phenylmethylsulfonylfluoride minus fluorine) indicated covalent binding of phenylmethylsulfonylfluoride to YahD. Spectra from native as well as phenylmethylsulfonylfluoride-reacted YahD displayed an additional peak with a mass gain of +208, which corresponds to the binding of sinapinic acid; this is a commonly observed artifact (Christoph Weise, pers. commun.).

To assess the hydrolytic function of YahD, we tested the hydrolytic activity of the enzyme on a wide range of substrates, covering all known functional classes of α/β hydrolases, namely *p*-nitrophenyl acetate, *p*-nitrophenyl butyrate, *p*-nitrophenyl palmitate, and 1-naphthyl acetate (carboxylesterase), *p*-methyl thiobutanoate and palmitoyl coenzyme A (thioesterase), polysorbate-20 and -80 (lipase), 4-methylumbelli feryl *p*-trimethyl ammoniocinnamate (feruloylesterase), *S*-lactoyl glutathione (glyoxalase II), 4-nitrophenyl phosphate, paraoxon-methyl (phosphoesterase), glycero-phosphoethanolamine (phospholipase C), L-α-phosphatidylcholine (phospholipase D), *N*-phenethylbutyramide (amidase), *p*-nitrostyrene oxide (epoxide hydrolase), mandelonitrile (hydroxynitrile lyase), peracetic acid (peroxoacid hydrolase) and dihydroxyacetone phosphate (methylglyoxal synthase). YahD did not hydrolyze any of these substrates under a range of conditions tested.

The presence of a malic acid molecule, which sterically resembles aspartic acid, in the active site of crystallized YahD spurred us to also test for protease and peptidase activity, including peptides that contained aspartate at the C- and N-terminus. The following peptidic substrates were tested: fluorescently labeled bovine serum albumin, bodipy-FL casein, gelatin, di- and tri-peptide libraries, Ala-Ala-Phe-7-amido-4-methylcoumarin, *N*-α-benzoyl-DL-arginine-4-nitroanilide, Asp-Ala-β-naphthylamide and Asp-β-naphthylamide. Again, no hydrolytic activity could be detected. An *L. lactis yahD* knockout mutant did not display a phenotype under a range of conditions tested, including copper stress, oxidative and nitrosative stress, sensitivity to methylglyoxal, formaldehyde, zeocin (acetyltransferase), mandelonitrile (hydroxynitrile lyase), methylcatechol (C–C bond hydrolase) and peracetic acid (data not shown).

Based on a BLAST search, YahD belongs to the family of esterases. However, with the massive increase of DNA sequences in the databases, combined with automated gene annotations, functional annotations have become compromised. Many methods have been developed in the last few years using sequential and structural data to gain functional clues, as reviewed elsewhere (Watson *et al.*, 2005). Such approximations have been used here. However, the experimentally characterized protein that is most closely related to YahD, a carboxylesterase from *P. fluorescens*, shares only 17%

sequence identity with YahD. This is hardly significant in the context of substrate specificity. Also, the α/β hydrolase fold is one of the most versatile and widespread folds known. Even though all the members of this superfamily have a similar fold and a conserved catalytic triad, they exhibit a wide range of substrate specificities. None of the substrates known to be hydrolyzed by esterases was a substrate for YahD. Similarly, other known α/β hydrolase substrates were not hydrolyzed by YahD. It appears likely that YahD represents a novel class of enzymes that evolved from the α/β hydrolase family to carry out a function that has not been characterized so far. An example of such an evolution of a novel function are the serine carboxypeptidase-like acyltransferases, which also possess an α/β hydrolase fold with a Ser-His-Asp catalytic triad, but evolved to catalyze a transacylation rather than a hydrolytic reaction (Steffens, 2000; Stehle *et al*., 2006). The fact that YahD is specifically induced by copper of course suggests a role in the defense against copper or associated stress conditions, but further work will be required to elucidate this novel cellular defense mechanism.

Acknowledgements

We are grateful to Rudolf Volkmer for providing peptides for the functional testing of YahD. We acknowledge access to beamline BL14.1 of the BESSY II storage ring (Berlin, Germany) via the Joint Berlin MX-Laboratory, sponsored by the Helmholtz Zentrum Berlin für Materialien und Energie, the Freie Universität Berlin, the Humboldt-Universität zu Berlin, the Max-Delbrück Centrum and the Leibniz-Institut für Molekulare Pharmakologie. This work was supported by grant 3100A0_122551 from the Swiss National Foundation, a grant from the International Copper Association, a grant from the Swiss State Secretary for Education & Research and by the DFG-Sonderforschungsbereich 449.

Authors' contributions

J.M. and S.M. contributed equally to this work.

References

Barré O, Mourlane F & Solioz M (2007) Copper induction of lactate oxidase of *Lactococcus lactis*: a novel metal stress response. *J Bacteriol* **189**: 5947–5954.

Bolotin A, Wincker P, Mauger S, Jaillon O, Malarme K, Weissenbach J, Ehrlich SD & Sorokin A (2001) The complete genome sequence of the lactic acid bacterium *Lactococcus lactis* ssp. *lactis* IL1403. *Genome Res* **11**: 731–753.

Brenner S (1988) The molecular evolution of genes and proteins: a tale of two serines. *Nature* **334**: 528–530.

Chillappagari S, Seubert A, Trip H, Kuipers OP, Marahiel MA & Miethke M (2010) Copper stress affects iron homeostasis by destabilizing iron–sulfur cluster formation in *Bacillus subtilis*. *J Bacteriol* **192**: 2512–2524.

Collaborative computational project, Number 4 (1994) The *CPC4* suite: Programs for protein crystallography. *Acta Cryst* **D50**: 760–763.

Emsley P & Cowtan K (2004) Coot: model-building tools for molecular graphics. *Acta Crystallogr D* **60**: 2126–2132.

Ermolaeva MD, White O & Salzberg SL (2001) Prediction of operons in microbial genomes. *Nucleic Acids Res* **29**: 1216–1221.

Guillot A, Gitton C, Anglade P & Mistou MY (2003) Proteomic analysis of *Lactococcus lactis*, a lactic acid bacterium. *Proteomics* **3**: 337–354.

Hong KH, Jang WH, Choi KD & Yoo OJ (1991) Characterization of *Pseudomonas fluorescens* carboxylesterase: cloning and expression of the esterase gene in *Escherichia coli*. *Agr Biol Chem* **55**: 2839–2845.

Kabsch W (1993) Automatic processing of rotation diffraction data from crystals of initially unknown symmetry and cell constants. *J Appl Crystallogr* **26**: 795–800.

Karlin KD (1993) Metalloenzymes, structural motifs, and inorganic models. *Science* **261**: 701–708.

Kim KK, Song HK, Shin DH, Hwang KY, Choe S, Yoo OJ & Suh SW (1997) Crystal structure of carboxylesterase from *Pseudomonas fluorescens*, an α/β hydrolase with broad substrate specificity. *Structure* **5**: 1571–1584.

Krissinel E & Henrick K (2007) Inference of macromolecular assemblies from crystalline state. *J Mol Biol* **372**: 774–797.

Laemmli UK & Favre M (1973) Maturation of the head of bacteriophage T4. *J Biol Chem* **80**: 575–599.

Linder MC & Hazegh Azam M (1996) Copper biochemistry and molecular biology. *Am J Clin Nutr* **63**: 797S–811S.

Liu Z, Gosser Y, Baker PJ *et al*. (2009) Structural and functional studies of *Aspergillus oryzae* cutinase: enhanced thermostability and hydrolytic activity of synthetic ester and polyester degradation. *J Am Chem Soc* **131**: 15711–15716.

Macomber L & Imlay JA (2009) The iron-sulfur clusters of dehydratases are primary intracellular targets of copper toxicity. *P Natl Acad Sci USA* **106**: 8344–8349.

Magnani D & Solioz M (2007) How bacteria handle copper. *Molecular Microbiology of Heavy Metals* (Nies DH & Silver S, eds), pp. 259–285. Springer, Heidelberg.

Magnani D, Barré O, Gerber SD & Solioz M (2008) Characterization of the CopR regulon of *Lactococcus lactis* IL1403. *J Bacteriol* **190**: 536–545.

Mermod M, Mourlane F, Waltersperger S, Oberholzer AE, Baumann U & Solioz M (2010) Structure and function of CinD (YtjD) of *Lactococcus lactis*, a copper-induced nitroreductase involved in defense against oxidative stress. *J Bacteriol* **192**: 4172–4180.

Murshudov GN, Vagin AA & Dodson EJ (1997) Refinement of macromolecular structures by the maximum-likelihood method. *Acta Crystallogr D* **53**: 240–255.

Nardini M & Dijkstra BW (1999) α/β hydrolase fold enzymes: the family keeps growing. *Curr Opin Struc Biol* **9**: 732–737.

Ollis DL, Cheah E, Cygler M, Dijkstra B, Frolow F, Franken SM, Harel M, Remington SJ, Silman I & Schrag J (1992) The α/β hydrolase fold. *Protein Eng* **5**: 197–211.

Sambrook J, Fritsch EF & Maniatis T (1989) *Molecular Cloning*. Cold Spring Harbor Laboratory Press, Cold Spring Harbor.

Simon GM & Cravatt BF (2010) Activity-based proteomics of enzyme superfamilies: serine hydrolases as a case study. *J Biol Chem* **285**: 11051–11055.

Solioz M & Stoyanov JV (2003) Copper homeostasis in *Enterococcus hirae*. *FEMS Microbiol Rev* **27**: 183–195.

Solioz M & Vulpe C (1996) CPx-type ATPases: a class of P-type ATPases that pump heavy metals. *Trends Biochem Sci* **21**: 237–241.

Solioz M, Abicht HK, Mermod M & Mancini S (2010) Response of Gram-positive bacteria to copper stress. *J Biol Inorg Chem* **15**: 3–14.

Solioz M, Mancini S, Abicht HK & Mermod M (2011) The lactic acid bacteria response to metal stress. *Stress Response of Lactic Acid Bacteria* (Papadimitriou K & Tsakalidou E, eds). Springer, Heidelberg, in press.

Steffens JC (2000) Acyltransferases in protease's clothing. *Plant Cell* **12**: 1253–1256.

Stehle F, Brandt W, Milkowski C & Strack D (2006) Structure determinants and substrate recognition of serine carboxypeptidase-like acyltransferases from plant secondary metabolism. *FEBS Lett* **580**: 6366–6374.

Stein N (2008) CHAINSAW: a program for mutating pdb files used as templates in molecular replacement. *J Appl Crystallogr* **41**: 641–643.

Terzaghi BE & Sandine WE (1975) Improved medium for lactic streptococci and their bacteriophages. *Appl Microbiol* **29**: 807–813.

Towbin H, Staehelin T & Gordon J (1979) Electrophoretic transfer of proteins from polyacrylamide gels to nitrocellulose sheets: procedure and some applications. *P Natl Acad Sci USA* **76**: 4350–4354.

Vagin A & Teplyakov A (2010) Molecular replacement with MOLREP. *Acta Crystallogr D* **66**: 22–25.

van de Guchte M, Serror P, Chervaux C, Smokvina T, Ehrlich SD & Maguin E (2002) Stress responses in lactic acid bacteria. *Antonie Van Leeuwenhoek* **82**: 187–216.

Watson JD, Laskowski RA & Thornton JM (2005) Predicting protein function from sequence and structural data. *Curr Opin Struc Biol* **15**: 275–284.